

Multijunction GaInP/GaInAs/Ge Solar Cells with Bragg Reflectors

V. M. Emelyanov[^], N. A. Kalyuzhniy, S. A. Mintairov, M. Z. Shvarts, and V. M. Lantratov

Ioffe Physical Technical Institute, Russian Academy of Sciences, St. Petersburg, 194021 Russia

[^]e-mail: resso2003@bk.ru

Submitted May 24, 2010; accepted for publication, May 28, 2010

Abstract—Effect of subcell parameters on the efficiency of GaInP/Ga(In)As/Ge tandem solar cells irradiated with 1-MeV electrons at fluences of up to $3 \times 10^{15} \text{ cm}^{-2}$ has been theoretically studied. The optimal thicknesses of GaInP and GaInAs subcells, which provide the best photocurrent matching at various irradiation doses in solar cells with and without built-in Bragg reflectors, were determined. The dependences of the photoconverter efficiency on the fluence of 1-MeV electrons and on the time of residence in the geostationary orbit were calculated for structures optimized to the beginning and end of their service lives. It is shown that the optimization of the subcell heterostructures for a rated irradiation dose and the introduction of Bragg reflectors into the structure provide a 5% overall increase in efficiency for solar cells operating in the orbit compared with unoptimized cells having no Bragg reflector.

DOI: 10.1134/S1063782610120122

1. INTRODUCTION

An important characteristic of multijunction space solar cells (SCs) is their stability against high-energy particles in the near-Earth space (protons, electrons, and γ -ray photons). These particles create additional nonradiative recombination centers in the SC structure. These centers cause a decrease in the diffusion length of minority charge carriers, which most strongly affects the photocurrents in subcells of multijunction SCs [1, 2]. In this study, we simulate the radiation damage to GaInP/GaInAs/Ge SCs comprising three subcells: GaInP, GaInAs, and Ge. The different rates of radiation degradation of the photocurrent in separate subcells disturbs the conditions of photocurrent matching between the subcells and impairs the efficiency of the multijunction SC. Therefore, to obtain maximum efficiency of a multijunction SC during its entire service life in the orbit, it is necessary to optimize the structure of its subcells, depending on the dose of particles that damage the SC in the course of its operation.

One of the ways to raise the radiation resistance of SCs is to use built-in Bragg reflectors (BRs) [3–5]. The BRs return a part of “long-wavelength” photons to the photoactive region with energy close to the band gap not absorbed in this region (Fig. 1). This makes it possible to diminish the thickness of photoactive layers and, accordingly, reduce the number of radiation defects in the structure. Unlike other methods for improving the radiation resistance, e.g., with lightly doped layers and dragging fields [6–11], this approach does not lead to a decrease in the height of potential barriers at $p-n$ junctions of the SC and in its open-circuit voltage. The Bragg reflector also serves as a rear potential barrier, which improves the collection of

minority charge carriers from the base region and favors an increase in the photocurrent.

The goal of our study was to attain the maximum radiation resistance of SCs by optimizing the heterostructures of the subcells of monolithic multijunction SCs GaInP/Ga_{0.99}In_{0.01}As/Ge with BRs for various irradiation doses.

2. A DECREASE IN PHOTOCURRENTS IN GaInP/GaInAs/Ge SOLAR CELLS UNDER IRRADIATION

The radiation damage to GaInP/GaInAs/Ge SCs was simulated with 1-MeV electrons because high-energy electrons are the main damaging factor in geo-synchronous orbits. The results obtained can be recalculated for other kinds of particles, depending on the material damage factors for these particles.

The decrease in the diffusion lengths of minority carriers upon irradiation of SCs with high-energy particles results in the subcell photocurrents of GaInP/GaInAs/Ge SCs becoming lower. The decrease in the diffusion length L for minority charge carriers is described by the following equation [12–15]:

$$\frac{1}{L^2} = \frac{1}{L_0^2} + \frac{1}{L_\phi^2}, \quad L_\phi = \sqrt{\frac{D}{K\phi}}, \quad (1)$$

where L is the diffusion length of minority charge carriers in a material, K is the material damage factor, ϕ is the fluence of damaging particles, L_0 is the diffusion length of minority charge carriers before irradiation, and D is the diffusion coefficient of minority charge carriers.

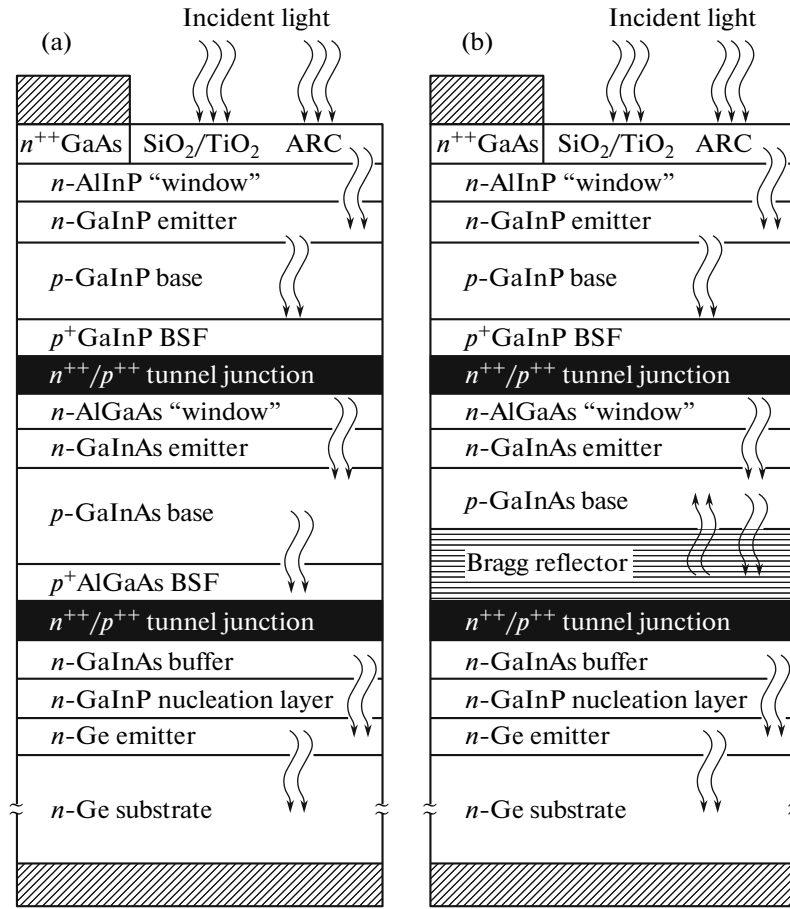


Fig. 1. Structures of the GaInP/GaInAs/Ge multijunction solar cells: (a) without and (b) with a Bragg reflector.

In addition to reducing the photocurrent, the decrease in the diffusion lengths of minority charge carriers in the emitter and base layers of the subcells leads to a lower open-circuit voltage. The open-circuit voltage of the j th subcell (before irradiation) is given in the case of a predominant recombination current in the $p-n$ junction by

$$V_{\text{oc}0}^{(j)} = \frac{2kT}{q} \ln \left(\frac{I_{\text{ph}}^{(j)}}{I_{\text{r}}^{(j)}} \right), \quad (2)$$

where k is the Boltzmann constant, T is the temperature, q is the elementary charge, $I_{\text{ph}}^{(j)}$ is the photocurrent density for the j th subcell, and $I_{\text{r}}^{(j)}$ is the recombination current density for the $p-n$ junction of the j th subcell calculated by the formula [16]

$$I_{\text{r}}^{(j)} = \frac{kTn_i \sqrt{D_n^{(j)} D_p^{(j)}}}{\Phi' L_n^{(j)} L_p^{(j)}} = I_{\text{r}0}^{(j)} \frac{L_{n0}^{(j)} L_{p0}^{(j)}}{L_n^{(j)} L_p^{(j)}}. \quad (3)$$

Here, $L_n^{(j)}$ and $L_p^{(j)}$ are the diffusion lengths of electrons and holes at the $p-n$ junction of the j th subcell, $D_n^{(j)}$

and $D_p^{(j)}$ are the diffusion lengths of charge carriers, n_i is the intrinsic charge-carrier concentration, Φ' is the average potential gradient in the $p-n$ junction, and $L_{n0}^{(j)}$, $L_{p0}^{(j)}$, and $I_{\text{r}0}^{(j)}$ are the diffusion lengths of carriers and recombination current density in the $p-n$ junction of the j th subcell before irradiation.

With (3) taken into account, the dependence of the open-circuit voltage on the carrier diffusion lengths at the $p-n$ junction of j th subcell under irradiation is expressed by the following formula:

$$V_{\text{oc}}^{(j)} = \frac{2kT}{q} \ln \left(\frac{I_{\text{ph}}^{(j)} L_n^{(j)} L_p^{(j)}}{I_{\text{r}0}^{(j)} L_{n0}^{(j)} L_{p0}^{(j)}} \right) = V_{\text{oc}0}^{(j)} - \frac{2kT}{q} \ln \left(\frac{L_{n0}^{(j)} L_{p0}^{(j)}}{L_n^{(j)} L_p^{(j)}} \right), \quad (4)$$

where $V_{\text{oc}0}^{(j)} = (2kt/q) \ln(I_{\text{ph}}^{(j)} / I_{\text{r}0}^{(j)})$ is the open-circuit voltage of the j th subcell before irradiation.

We used expression (2) to calculate the diffusion lengths of minority charge carriers in the emitters and bases of the GaInP, GaInAs, and Ge subcells of the triple-junction $n-p$ -GaInP/GaInAs/Ge SC for irradiation with 1-MeV electrons at fluences in the range from zero to $3 \times 10^{15} \text{ cm}^{-2}$. The parameters used in this

Table 1. Parameters for calculation of the minority charge-carrier diffusion lengths in the photoactive layers of the subcells of the GaInP/GaInAs/Ge SC

Layer	Value of a parameter		
	K , $\text{cm}^2 \text{s}^{-1}$	D , $\text{cm}^2 \text{s}^{-1}$	dopant concentration, 10^{17} cm^{-3}
<i>n</i> -GaInP	3.6×10^{-7} [19]	5	100
<i>p</i> -GaInP		50	1
<i>n</i> -GaInAs	1.2×10^{-6} [19]	7	20
<i>p</i> -GaInAs		65	4
<i>n</i> -Ge	1.2×10^{-10} [19]	30	1–100
<i>p</i> -Ge		80	2

Table 2. Calculated diffusion lengths of minority charge carriers in the photoactive layers of the GaInP/GaInAs/Ge SC

Layer	Diffusion length of minority charge carriers, μm		
	Before irradiation	After irradiation with 1-MeV electrons	
		irradiation dose $10^{15}, \text{cm}^{-2}$	irradiation dose $3 \times 10^{15}, \text{cm}^{-2}$
<i>n</i> -GaInP		0.05	
<i>p</i> -GaInP	2	1.76	1.46
<i>n</i> -GaInAs	0.3	0.28	0.25
<i>p</i> -GaInAs	7	2.21	1.31
<i>n</i> -Ge	—	0.5	—
<i>p</i> -Ge	50	49.1	47.4

calculation are listed in Table 1. The calculated diffusion lengths in the SC layers before and after irradiation with electrons at fluences of 10^{15} and $3 \times 10^{15} \text{ cm}^{-2}$

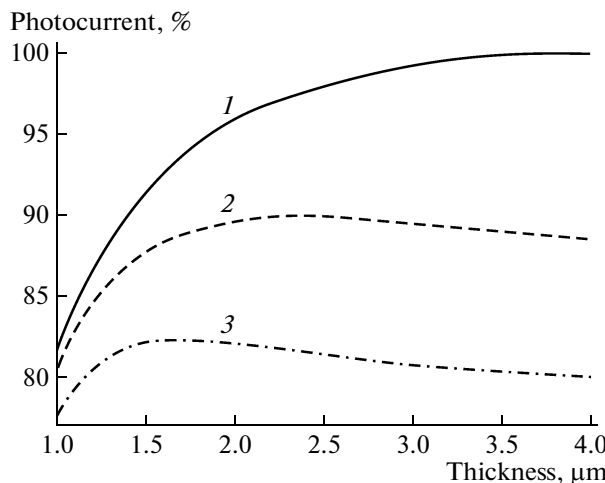


Fig. 2. Fraction of the photocurrent generated in a GaInAs subcell without Bragg reflectors (1) before and (2, 3) after irradiation with 1-MeV electrons at a dose of (2) 10^{15} and (3) $3 \times 10^{15} \text{ cm}^{-2}$. The thickness of the *n*-GaInAs emitter was $0.1 \mu\text{m}$.

are listed in Table 2. The calculated values of the diffusion length before irradiation are in agreement with those determined in [17, 18].

The data in Table 2 show that the strongest degradation is observed for the GaInAs subcell, for which the diffusion length of minority charge carriers in the base decreases from 7 to $1.31 \mu\text{m}$. The decrease in the diffusion length of minority charge carriers in the *p*-base of GaInP has no significant effect on the photocurrent degradation in the subcell because the diffusion length of $1.46 \mu\text{m}$ is sufficient for providing complete collection of photogenerated carriers [17].

In this study, we optimized the GaInAs subcell, which is the most strongly degraded under exposure to radiation, and the GaInP subcell in order to match the subcells in the photocurrent in the GaInP/GaInAs/Ge SC. Since the photocurrent in the Ge subcell commonly markedly exceeds the photocurrents of the rest of the subcells and does not limit the short-circuit current of the multijunction SC, it was not optimized.

3. OPTIMIZATION OF GaInP AND GaInAs SUBCELLS

The diffusion lengths calculated for various materials for prescribed fluences of irradiation with 1-MeV electrons were used to simulate spectral characteristics of GaInP/GaInAs/Ge SCs and to calculate the photocurrents of their subcells. The simulation was performed using the method considered in [17]. The refractive indices and absorption coefficients of semiconducting materials, used in the calculation, were taken from [21, 22].

Figure 2 shows the calculated dependences of the fraction of the photocurrent generated in the GaInAs on its thickness. Prior to irradiation, a nearly 100% collection of carriers is achieved at a subcell thickness of $4 \mu\text{m}$ (Fig. 2, curve 1). The photocurrent of the subcell becomes lower upon irradiation because of a decrease in the diffusion length of minority charge carriers in the base of *p*-GaInAs (Fig. 2, curves 2, 3). In this case, the maximum photocurrent is reached at a smaller subcell thickness as the irradiation dose is raised. However, the number of long-wavelength photons not absorbed in the thin base increases as its thickness decreases.

The fraction of absorbed light can be raised at a decreasing subcell thickness by using a BR to return part of the long-wavelength light to the photoactive layers. Two BR designs were suggested in [5]: single-section, comprising 20 pairs of $\text{Al}_{0.1}\text{Ga}_{0.9}\text{As}$ ($59 \pm 1 \text{ nm}$)/AlAs ($72 \pm 1 \text{ nm}$) layers providing the maximum reflection at a wavelength of 860 nm , and double-section, containing, in addition to these 20 pairs of layers, additional 20 pairs of $\text{Al}_{0.2}\text{Ga}_{0.8}\text{As}$ ($54 \pm 1 \text{ nm}$)/AlAs ($64 \pm 1 \text{ nm}$) layers providing the maximum reflection at a wavelength of 770 nm . The single-

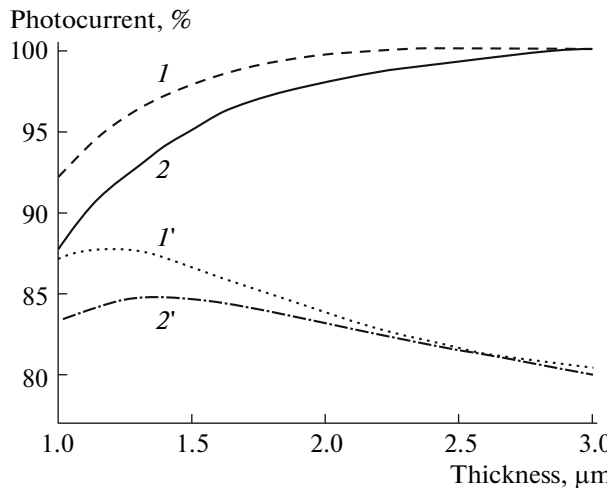


Fig. 3. Calculated photocurrent generated in GaInAs subcells of various thicknesses, with Bragg reflectors of two designs: (1, 1') double-section BR before and after irradiation with 1-MeV electrons at a dose of $3 \times 10^{15} \text{ cm}^{-2}$ and (2, 2') single-section BR before and after irradiation.

and double-section BRs provide an effective reflection of light in the spectral ranges 800–900 and 750–900 nm, respectively.

The variation in the photocurrents generated by GaInAs subcells having BRs with the thickness of photoactive layers before and after electron irradiation is shown in Fig. 3. In structures with BRs, the maximum photocurrent is obtained at smaller layer thicknesses and the photocurrent at the point of maximum is 2–5% higher than that in a structure without BRs under similar irradiation conditions (Fig. 2).

The GaInAs subcell thickness providing the maximum photocurrent at a given irradiation dose can be taken to be the optimal value. Figure 4 shows dependences of the optimal thickness of the GaInAs subcell on the electron fluence. It can be seen that use of BRs leads to a decrease in the optimal thicknesses of the subcells, which improves their radiation resistance. The relative change in the optimal thickness with increasing fluence of damaging particles is also smaller in this case.

The optimal thickness of the GaInP subcell was chosen on the basis of the condition for photocurrent matching of the GaInP and GaInAs subcells in the GaInP/GaInAs/Ge SC at a fluence of 1-MeV electrons (Fig. 4). As the electron fluence increases, the optimal thickness of the GaInP subcell decreases to provide a higher transmission of light into the GaInAs subcell. The optimal thicknesses for cells with BRs are larger because the better radiation hardness of the GaInAs subcells in these SCs makes it possible to raise the thickness of GaInP layers and obtain a higher photocurrent.

The double-section BR provides a better radiation resistance of SCs, compared with the single-section

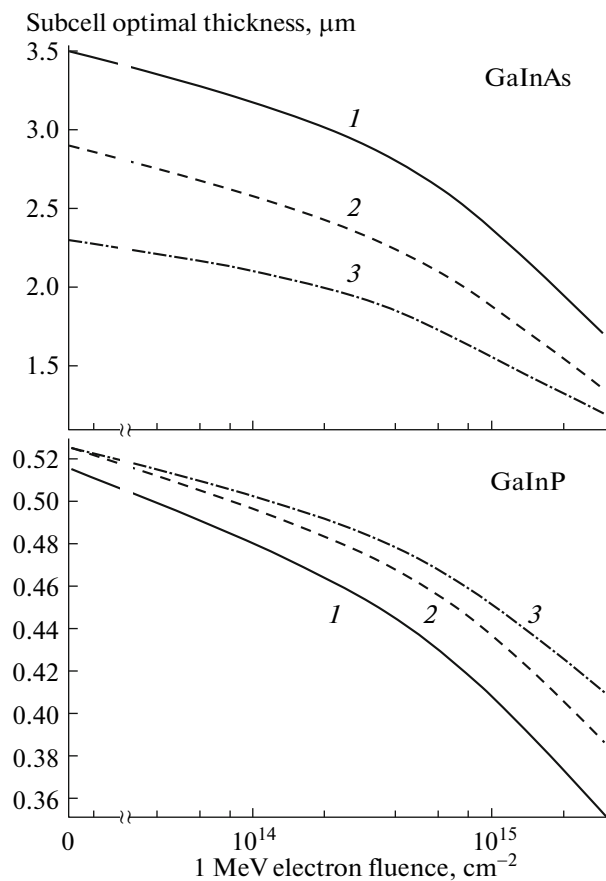


Fig. 4. Calculated optimal thicknesses of the GaInAs and GaInP subcells at various doses of 1-MeV electrons in GaInP/GaInAs/Ge SCs of three designs: (1) without a BR, (2) with a single-section BR, and (3) with a double-section BR.

BR [5]. Therefore, to estimate the optimization efficiency, we calculated dependences of the short-circuit current and the efficiency of SCs without BRs and with a double-section BR on the fluence of 1-MeV electrons and on the corresponding residence time of photocells in the geosynchronous orbit for various thicknesses of the GaInP and GaInAs subcells (Figs. 5, 6). It can be seen that, in the range under consideration, the short-circuit current of an SC optimized for a rated fluence of $3 \times 10^{15} \text{ cm}^{-2}$ of 1-MeV electrons hardly decreases and also has the maximum value at the end of its service life (Fig. 5, curves 3, 3'). At the same time, the current of the SCs optimized for a rated fluence of 10^{15} cm^{-2} of 1-MeV electrons (Fig. 5, curves 2, 2') is higher than that of the former up to an electron fluence of $1.5 \times 10^{15} \text{ cm}^{-2}$ and shows only a slight decrease at higher fluences. In this case, the use of BRs makes it possible to obtain a 0.5- to 1-mA cm^{-2} -higher short-circuit current of a multijunction cell compared with SCs without a BR for all the SC types considered.

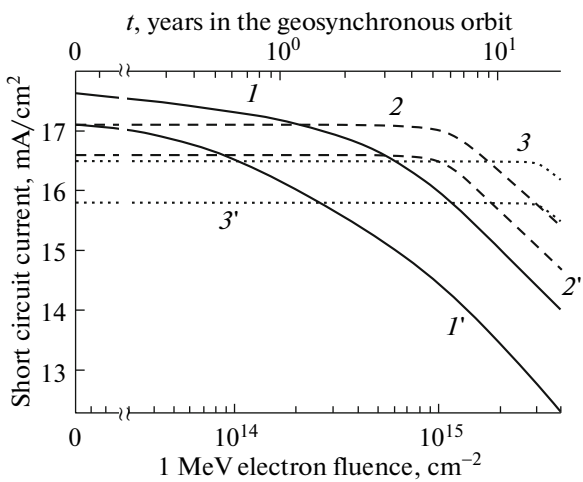


Fig. 5. Calculated variation (with the irradiation dose) in the short-circuit current in GaInP/GaInAs/Ge SCs ($1'$, $2'$, $3'$) without BR and (1 , 2 , 3) with a double-section BR for different 1-MeV electron doses to which the SC structures were optimized: (1 , $1'$) 0 , (2 , $2'$) 10^{15} , and (3 , $3'$) $3 \times 10^{15} \text{ cm}^{-2}$.

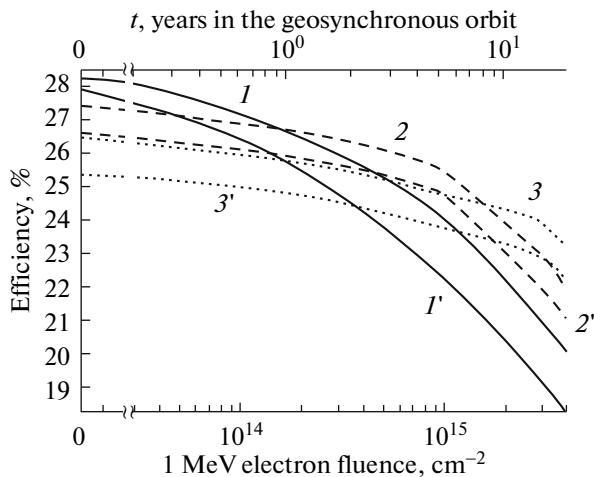


Fig. 6. Calculated variation in the efficiency with the irradiation dose under the AM0 conditions of GaInP/GaInAs/Ge SCs ($1'$, $2'$, $3'$) without BR and (1 , 2 , 3) with a double-section BR for different 1-MeV electron doses to which the SC structures were optimized: (1 , $1'$) 0 , (2 , $2'$) 10^{15} , and (3 , $3'$) $3 \times 10^{15} \text{ cm}^{-2}$.

The decrease in the cell efficiency is accounted for by a decrease both in the photocurrent and in the open-circuit voltage. The elements the structures of which were optimized for the beginning of their operation in the orbit have the maximum initial efficiency but degrade at the highest rate. The decrease in the efficiency of the SCs the structures of which were optimized to a 10^{15} cm^{-2} dose of 1-MeV electrons is due to the fall of the open-circuit voltage at lower irradiation doses and, only after this value is reached, to the decrease in the short-circuit current. The degradation

of SCs optimized to a dose of 3×10^{15} of 1-MeV electrons is fully accounted for by the fall of the open-circuit voltage. It can be seen that, as also in the case of the short-circuit current, the highest efficiency at electron doses of 2×10^{14} to $(1.5-2) \times 10^{15} \text{ cm}^{-2}$ is observed for the structure optimized for the rated dose of 10^{15} cm^{-2} . At larger irradiation doses, the highest efficiency is observed for the structure optimized to an electron dose of $3 \times 10^{15} \text{ cm}^{-2}$, and at smaller doses, for that optimized to the beginning of operation.

4. CONCLUSIONS

In this study, the effect of subcell thicknesses in a GaInP/GaInAs/Ge SC on its short-circuit current and efficiency at various degrees of radiation damage was examined.

It was shown that the degradation of multijunction monolithic SCs optimized to the end of the operation life is substantially weaker than that for SCs optimized to its beginning. The difference in efficiency between these two groups of SCs may reach a value exceeding 3% by the end of the operation life. The cause of this is that the decline of the efficiency of SCs optimized to the final period of their operation is largely determined by the decrease in the open-circuit voltage, whereas the short-circuit current of a multijunction cell remains constant until a certain instant of time. Use of BRs gives an additional 0.5–2% gain in efficiency at various extents of radiation damage, compared with structures without a BR. In this case, the total increase in efficiency upon optimization of heterostructures to a rated irradiation dose and introduction of a BR reaches a value of 5%.

The choice of layer thicknesses that are optimal for large irradiation doses leads to a lower initial efficiency, but makes it possible to diminish the rate of degradation of an SC and to provide a higher output electric power, beginning from a certain instant of time after its being launched into orbit. For solar cells optimized to a fluence of 10^{15} cm^{-2} of 1-MeV electrons, this instant of time comes in less than a year after the beginning of operation. After three years in geosynchronous orbit, solar cells optimized to a fluence of $3 \times 10^{15} \text{ cm}^{-2}$ of 1-MeV electrons will have a higher efficiency, compared with photoconverters optimized at the beginning of their operation life.

SCs with double-section BRs optimized to the maximum electron fluence of 10^{15} cm^{-2} are preferable in operation in geosynchronous orbit for up to ten years. At longer durations of active operation, SCs with a double-section BR should be used, with their structures optimized to the maximum electron fluence of $3 \times 10^{15} \text{ cm}^{-2}$ or more. However, SCs of this kind will have a lower efficiency at the beginning of the flight.

ACKNOWLEDGMENTS

This study was supported by the Russian Foundation for Basic Research, projects nos. 08-00916-a, 09-08-00879-a, and 09-08-00954-a.

REFERENCES

1. M. Meusel, C. Baur, W. Guter, M. Hermle, F. Dimroth, A. W. Bett, T. Bergunde, R. Dietrich, R. Kern, W. Kossteller, M. Nell, W. Zimmermann, G. LaRoche, G. Strobl, S. Taylor, C. Signorini, and G. Hey, in *Proc. of the 20th EPSEC* (Barcelona, 2005), p. 20.
2. T. Sumita, M. Imaizumi, S. Matsuda, T. Ohshima, A. Ohi, and T. Kamiya, in *Proc. of the 3rd WCPVEC* (2003), p. 689.
3. V. M. Lantratov, I. V. Kochnev, and M. Z. Shvarts, in *Proc. of the 27th SOTAPOLCS Electrochemical Society*, vol. 97–21, p. 125.
4. M. Z. Shvarts, O. I. Chosta, I. V. Kochnev, V. M. Lantratov, and V. M. Andreev, *Sol. Energy Mater. Solar Cells* **68**, 105 (2001).
5. V. Emelyanov, N. Kaluzhniy, S. Mintairov, M. Shvarts, and V. Lantratov, in *Proc. of the Intern. Conf. on Micro- and Nano-Electronics 2009* (SPIE, Bellingham, WA, 2010), Proc. SPIE **7521**, 75210D (2010).
6. V. M. Andreev, V. S. Kalinovskii, O. V. Sulima, et al., *Fiz. Tekh. Poluprovodn.* **22**, 881 (1988) [Sov. Phys. Semicond. **22**, 556 (1988)].
7. K. A. Bertness, M. L. Ristow, M. E. Klausmeier-Brown, M. Grounner, M. S. Kuryla, and M. S. Werthen, in *Proc. of the 21st IEEE PVSC* (Kissimmee, FL, 1990), p. 1231.
8. K. A. Bertness, B. T. Cavicchi, S. R. Kurtz, J. M. Olson, A. E. Kibbler, and C. Kramer, in *Proc. of the 22nd IEEE PVSEC* (Las Vegas, NV, 1991), p. 1582.
9. V. P. Khvostikov, V. R. Larionov, E. V. Paleeva, S. V. Sorokina, O. I. Chosta, M. Z. Shvarts, and N. S. Zimogorova, in *Proc. of the 4th Eur. Space Power Conf.* (Poitiers, France, 1995), v. 2, p. 359.
10. V. M. Andreev, V. S. Kalinovskii, and O. V. Sulima, in *Proc. of the 10th EPVSEC* (Lisbon, 1991), p. 52.
11. O. I. Chosta, V. P. Khvostikov, V. M. Lantratov, and M. Z. Shvarts, in *Proc. of the 14th EPVSEC* (Barcelona, 1997), p. P6 A.14.
12. J. Loferski and P. Rappaport, *J. Phys. Rev.* **111**, 432 (1957).
13. F. Junga and A. Enslow, *IRE Trans. NS-6*, 49 (1959).
14. W. Rosenzweig, H. K. Gummel, and F. M. Smits, *Bell Syst. Techn. J.* **42**, 399 (1963).
15. W. Rosenzweig, F. M. Smits, and W. L. Brown, *J. Appl. Phys.* **35**, 2707 (1964).
16. A. M. Vasil'ev and A. P. Landsman, *Semiconductor Phototransducers* (Sov. radio, Moscow, 1971) [in Russian].
17. V. M. Emel'yanov, S. A. Mintairov, N. A. Kaluzhniy, and V. M. Lantratov, *Nauchno-Tekh. Vedom. SPbGPU: Fiz. Mat.* **77**, 14 (2009).
18. S. A. Mintairov, V. M. Andreev, V. M. Emel'yanov, N. A. Kaluzhniy, N. K. Timoshina, M. Z. Shvarts, and V. M. Lantratov, *Fiz. Tekh. Poluprovodn.* **44**, 1118 (2010) [Semiconductors **44**, 1084 (2010)].
19. M. Yamaguchi, T. Sasaki, H.-S. Lee, C. Morioka, N. J. Ekins-Daukes, M. Imaizumi, T. Takamoto, and T. Ohshima, in *Proc. of the 33rd IEEE PVSC* (San Diego, USA, 2008), PVSC.2008.4922716.
20. S. Sato, H. Miyamoto, M. Imaizumi, K. Shimazaki, C. Morioka, K. Kawano, and T. Ohshima, in *Proc. of the 33rd IEEE PVSC* (San Diego, USA, 2008), PVSC.2008.4922706.
21. D. E. Aspnes, S. M. Kelso, R. A. Logan, and R. Bhat, *J. Appl. Phys.* **60**, 754 (1986).
22. S. S. Adachi, *Optical Constants of Crystalline and Amorphous Semiconductors: Numerical Data and Graphical Information* (Kluwer Academic, Boston, 1999).

Translated by M. Tagirdzhanov